

A clumped-foilage canopy radiative transfer model for a global dynamic terrestrial ecosystem model. I: Theory

Wenge Ni-Meister^{a,*}, Wenze Yang^a, Nancy Y. Kiang^b

^a Department of Geography, Hunter College of The City University of New York, 695 Park Ave., New York, NY 10065, United States

^b NASA Goddard Institute for Space Studies, New York, NY, United States

ARTICLE INFO

Article history:

Received 25 June 2009

Received in revised form 23 February 2010

Accepted 23 February 2010

Keywords:

Canopy radiative transfer

Clumping

Heterogeneity

ABSTRACT

This study develops a simple but physically based canopy radiative transfer scheme for photosynthesis, radiative fluxes and surface albedo estimates in dynamic global vegetation models (DGVMs), and particularly for the Ent Dynamic Global Terrestrial Ecosystem Model (Ent DGTEM). The Ent DGTEM can represent vegetation in mixed as opposed to homogeneous canopies. With active growth and competition, it must predict radiative transfer for dynamically changing vegetation structure, and requires computational speed for coupling with atmospheric general circulation models (GCMs). The canopy radiative transfer scheme accounts for both vertical and horizontal heterogeneity of plant canopies by combining the simple two-stream scheme with a well-described actual vertical foliage profile, an analytically derived foliage clumping factor from geometric optical theory, and, for needleleaf trees, an empirical needle-to-shoot-clumping factor. In addition, the model accounts for the effect of trunks, which is significant in bare canopies. This model provides better radiation estimates (light profiles, albedo) than the two-stream scheme currently being used in most GCMs to describe light interactions with vegetation canopies. This scheme has the same computational cost as the current typical scheme being used in GCMs, but promises to provide better canopy radiative transfer estimates for DGVMs, particularly those that model heterogeneous vegetation canopies.

© 2010 Elsevier B.V. All rights reserved.

1. Introduction

Calculation of canopy radiative transfer for simulation of coupled biosphere–atmosphere interactions, such as in atmospheric general circulation models (AGCMs) must be able to provide: (1) the albedo of the vegetated land surface for the atmospheric model's energy balance, (2) the vertical profile of incident radiation on foliage through the vegetation canopy for estimating photosynthesis and stomatal conductance as controllers of land surface fluxes, and (3) the penetration of radiation to the ground to predict soil temperature and snowmelt. The transmission of light through plant canopies results in vertical profiles of light intensity that affect the photosynthetic activity and gas exchange of plants, their competition for light, and the canopy energy balance. The accurate representation of the canopy light profile is then important for predicting ecological dynamics. The level of detail at which this canopy radiative transfer should be described depends on how precisely one wishes to address the above problems, how structurally complex the canopy is, the availability of data for parameters at

the spatial scale of application, and finally the computational constraints of the modeling environment.

In the land biosphere component of these models, the representation of vegetation structure has been as homogeneous canopies of single vegetation types, with mosaicked cover types to represent subgrid heterogeneity at the global scale (Matthews, 1983; Sellers et al., 1996; Cox, 2001; Bonan et al., 2002; Sitch et al., 2003; Levis et al., 2004). More recently, efforts to improve the representation of vegetation community and ecological dynamics have introduced models of mixed canopies of dynamically changing structure, particularly the Ecosystem Demography (ED) model of Moorcroft et al. (2001), which has been applied at regional scales. The Ent dynamic global terrestrial ecosystem model (DGTEM) (Kiang et al., 2006) is the first model to take the ED approach specifically for coupling with GCMs. Dynamically changing mixed canopies call for a canopy radiative transfer scheme that accounts for the spatial heterogeneity in their foliage and stem elements, a scheme that also must be computationally fast. We present here a canopy radiative transfer scheme geared specifically for the development of the Ent DGTEM, but general enough with respect to common canopy geometry parameters that it should be useful for other state-of-the-art DGTEMs or dynamic global vegetation models (DGVMs).

The amount of radiation absorbed, reflected, and transmitted in plant canopies depends on the beam fraction of incident radiation,

* Corresponding author. Tel.: +1 212 772 5321; fax: +1 212 772 5268.
E-mail address: Wenge.Ni-Meister@hunter.cuny.edu (W. Ni-Meister).

Nomenclature

Roman alphabet

$a, a_1 - a_{10}$	coefficients of two-stream solution
$A_{sha}(L')$	radiation absorption per unit shaded leaf area
$A_{sun}(L')$	radiation absorption per unit sunlit leaf area
$A_{tot}(L')$	absorption
b	vertical crown radius (m)
D	crown diameter (m)
DBH	trunk diameter at breast height (m)
F_a	foliage area volume density of a single crown (m^{-1})
f_{sha}, f_{sl}	fraction of shaded and sunlit leaf
$G(\theta)$	leaf orientation function
h	crown center height within the canopies (m)
h_1, h_2	lower and upper bound of the crown centers (m)
I^\uparrow, I^\downarrow	upward and downward diffuse radiative fluxes normalized by the incident radiation flux density
$I_b^\uparrow, I_b^\downarrow$	upward and downward diffuse radiative normalized fluxes as incident radiation contains direct sunlit beam
$I_d^\uparrow, I_d^\downarrow$	upward and downward diffuse radiative normalized fluxes as incident radiation contains only diffuse light
I_b	fraction of incident sunlit beam
I_d	fraction of incident diffuse light
$L(z)$	cumulative leaf area index (LAI), from canopy top to height z
L_t	total LAI, from canopy top to bottom
$L_e(z)$	total projected accumulative effective LAI at height z
$L_{ei}(z)$	projected accumulative effective LAI for i th layer at height z
$L'(z)$	effective LAI, as the product of clumping factor and LAI
$p(s 1)$	path length distribution for light rays passing through one crown
$P_n(\theta)$	gap probability of light rays passing through n crowns, given θ
$P_{gap}(z, \theta)$	gap probability for light passing through the whole canopy
$P_{trk}(z, \theta)$	between-trunk probability
$q(r)$	proportion of the light striking the sphere of radius r that will pass through the canopy without interception
r	horizontal crown radius (m)
$R(L)$	reflectance
$S(\theta)$	crown projected area on the ground along the ray direction with the incident zenith angle θ (m^2)
$S_{trk}(z, \theta)$	projected mean trunk area (m^2)
s	distance traveled by a photo within the canopy (m)
$s n$	path length given that a photon will penetrate n individual canopies (m)
\overline{STAR}	hemispherically averaged silhouette to total area ratio
$T(L)$	transmittance
V	crown volume (m^3)
z	canopy height variable (m)

Greek alphabet

α	land surface albedo
β, β_0	up-scatter coefficients for diffuse and direct beam radiation
γ	clumping factor
γ'	clumping factor for conifer forest

γ_E	needle-to-shoot ratio
θ	solar zenith angle ($^\circ$ or rad)
τ_0	attenuation parameter (m^{-1})
λ	crown count density (m^{-2})
Γ	adjusting factor to convert path length s from spherical space into ellipsoidal space
$\bar{\mu}$	average inverse diffuse optical depth per unit leaf area
ω	leaf scattering coefficient
ω_N	needle scattering coefficient
ω_{sh}	shoot scattering coefficient
κ	extinction coefficient for direct beam radiation
σ	constant for two-stream solution
ρ_s	background albedo

canopy structure, the optical properties of the plant elements, and the albedo of the underlying soil/snow surface (Ross, 1981). Models of canopy radiative transfer range from the very simple Beer's Law exponential extinction of light through homogeneous, closed canopies (Ross, 1975) to detailed geometric optical and radiative transfer models that treat mixtures of individual trees, and multiple scattering with foliage clumped within tree crowns (Li et al., 1995; Ni et al., 1997) and along shoots (Wang and Jarvis, 1990a; Oker-Blom et al., 1991; Leblanc et al., 2005), and heterogeneously within tree crowns (Wang et al., 1990; Wang and Jarvis, 1990b). Observations and the detailed geometric models demonstrate that clumping of foliage is a significant factor affecting the vertical light profile in many canopies, such as needleleaf forest and savannas and, in general, in forest canopies that are not completely closed (Nilson, 1971, 1992; Cescatti, 1997a,b; Chen, 1996; Jupp, 2004; Kucharik et al., 1999; Yang et al., 2001; Wang and Jarvis, 1993; Valladares and Guzman, 2006; Jonckheere et al., 2004; Chen et al., 2008). Foliage clumping has been shown to be significant for accurate calculation of albedo (Ni and Woodcock, 2000), absorbed photosynthetically active radiation (Asrar et al., 1992; Chen et al., 2008), photosynthesis and canopy conductance (Law et al., 2001; Walcroft et al., 2005; Davi et al., 2006; Mo et al., 2008), the land surface energy balance (Anderson et al., 2005) and the timing of snowmelt (Hardy et al., 1997).

In most of the current land surface biophysical and biogeochemical process models implemented in GCMs, it is assumed that the canopy is homogeneous. The two-stream scheme, an analytical scheme of radiative transfer theory, is the most popular scheme being used in GCMs (Dickinson, 1983; Sellers, 1985; Bonan, 1996). For most natural woody vegetation, such as conifer forests, deciduous forest, savanna/woodland/shrubland, various sizes of gaps exist between different tree crowns, and the two-stream scheme results in errors in estimating photosynthetically active radiation (PAR), surface albedo and other radiative fluxes such as longwave radiation for canopy leaf temperature estimates.

The amount of radiation absorbed, transmitted, and reflected through a forest canopy is influenced by all the aboveground plant elements: leaves, needles, stems, branches and trunks and their spatial positions and orientations (Ross, 1975). To characterize the spatial clumping of vegetation structure on radiation regime, Nilson (1971) and Chen and Black (1991) introduced a clumping factor, γ , to Beer's Law to characterize the plant canopy gap fraction, i.e.:

$$P_{gap}(\theta) = \exp\left(\frac{-\gamma G(\theta)L_t}{\cos(\theta)}\right) \quad (1)$$

where $P_{gap}(\theta)$ is transmittance; θ is the solar zenith angle; G is a leaf orientation function (Sellers, 1985); and L_t is the leaf area

index; γ is the clumping factor. When $\gamma = 1$, then, of course, there is no clumping and leaves are randomly distributed. When $\gamma < 1$, the beam transmission is enhanced by clumping. When $\gamma > 1$, then leaves are more uniformly distributed. Chen (1996) and Smolander and Stenberg (2003) also introduced a needle-to-shoot area ratio to quantify the clumping of needles into shoots for conifer forest.

Chen and Cihlar (1995) present a method to estimate the clumping factor based on the gap size distribution, which could be measured using the Tracing Radiation and Architecture of Canopies (TRAC) instrument. Kucharik et al. (1999) presented a method to estimate the clumping factor semi-empirically as:

$$\gamma(\theta) = \frac{(N \cdot D/\sqrt{B})^{0.7}}{1 + b \exp(k\theta^p)}, \quad (2)$$

where N is the number of stems in an area B ; D is the crown diameter; p , k and b are estimated through fitting or Monte Carlo simulation.

The work mentioned above used a fitted clumping factor in Beer's Law to characterize the effect of horizontal vegetation structure on the radiation regime and to estimate gap fraction at the bottom of the canopy. To characterize the vertical variation of the light profile, Ni et al. (1997) used a full Geometric Optical and Radiative Transfer (GORT) model. Through fusion of the geometric optics and radiative transfer theory, GORT characterizes the effect of both the horizontal and vertical vegetation heterogeneity on canopy radiation regime within forest canopies. Unlike two-stream schemes that rely simply on total leaf area index (LAI) and leaf angle distribution functions, GORT takes into account statistical characterization of tree geometry and community structure, including crown width and depth, variation in tree height, and tree density. Several DGVMs coupled to GCMs predict these variables through growth dynamics of mosaicked homogeneous canopies (Community Land Model's DGVM by Levis et al., 2004; Lund-Potsdam-Jena by Sitch et al., 2003; ORCHIDEE by Krinner et al., 2005). The ED and Ent DGTEMs predict these variables for dynamic mixed communities. Therefore, the theory behind GORT is very compatible for use with GCM-coupled DGVMs, and especially for describing mixed canopies. However, the computational cost would be too high to run full GORT at the global scale.

Therefore, the overall purpose of this study is to develop a computationally fast, analytical geometric optical and radiative transfer scheme to account for the effect of 3D heterogeneous vegetation structure on the light regime in forest canopies for dynamic global vegetation models (DGVMs), particularly those coupled to GCMs. Section 2 presents the full theoretical model development including subcomponents of (a) analytical expressions for canopy vertical gap probability with the clumping factor (needle-to-shoot level, leaf to crown level), vertical foliage and stem profiles for single layer and multilayered canopies based on geometric optics; and (b) calculation of absorbed, transmitted, and reflected radiative components through fusion of this canopy gap probability with the

Table 2
Spectral properties of leaf types and backgrounds used in this study.

Wavelength (μm)	0.3–0.74	0.74–1.35	1.35–4.0	Sources
Broadleaf albedo	0.15	0.8	0.35	Sellers et al. (1996)
Needleleaf albedo	0.12	0.45	0.45	Sellers et al. (1996)
Soil albedo	0.075	0.314	0.13	Ni and Woodcock (2000)
Snow albedo	0.939	0.787	0.0	Ni et al. (1997)

two-stream scheme. Section 3 presents simulation of sensitivity studies and Section 4 presents discussion and conclusions.

This paper develops the theoretical mathematical framework for our canopy radiative transfer model, presenting sensitivity to different kinds of canopy structures, taking realistic parameter values from actual forests. Tables 1 and 2 list all inputs used in our runs in this study. Note that these are only to illustrate theoretical sensitivities, while a full evaluation against measured light transmittance is presented in a companion paper, Yang et al. (2010).

2. Model development

Our modeling approach was to derive an analytical version of the GORT model to calculate canopy gap probabilities as functions of leaf properties, tree geometry and density. This involves modeling both the vertical foliage profile and horizontal clumping of foliage. We couple these expressions of canopy gap probability with a two-stream scheme. The predictions of vertical light profiles, canopy albedo, and transmittance to the ground are compared to those of the full GORT model.

GORT was developed to describe the effects of three-dimensional canopy structure on the radiation environment and to characterize the heterogeneous radiation environment in natural vegetation at the forest stand scale (Li et al., 1995). Merging theory from geometric optics and radiative transfer, the GORT model treats vegetation canopies as assemblages of randomly distributed tree crowns of ellipsoidal shape. The tree crowns are filled with leaves that absorb and scatter radiation passing through the crown (Fig. 1). Principles of radiative transfer are used in describing the multiple scattering of leaves inside crowns and the multiple scattering among crowns and the ground surface. The GORT model has been used successfully in describing the bidirectional reflectance distribution function (BRDF) characteristics of forests, including the "hotspot," and was extended by Ni et al. (1997) to include the vertical canopy gap probability profile. It deals with multilayer and multispecies vegetation canopies through convolution of mixed communities (Ni-Meister et al., 2001, 2008). New addition to GORT recently was to characterize impacts of branches and trunks on the radiation environment analytically (Ni-Meister et al., 2008). The trunk is modeled in a cylinder shape below a crown and a cone or cylinder shape within a crown (Fig. 1).

GORT has proven very useful in a variety of applications. It has been successfully used to model photosynthetically active radiation

Table 1
Canopy geometric structure parameters^a used in this study.

Figure no./sources	Subsite	r (m)	b (m)	λ (m^{-2}) ^b	P_a ($\text{m}^2 \text{m}^{-3}$) ^c	h_1 (m)	h_2 (m)	DBH (m)	b/r	PAI
Figs. 2, 8, 11 and 12 (Yang et al., 2010) ^d	Leaf-on—upper	3.17	3.39	0.068	0.343	13.81	23.82	0.223	1.07	3.30
	Leaf-on—lower	2.00	1.27	0.145	0.455	4.18	5.55	0.087	0.63	1.40
	Leaf-off—upper	3.17	3.39	0.068	0.038	13.81	23.82	0.223	1.07	0.36
	Leaf-off—lower	2.00	1.27	0.145	0.045	4.18	5.55	0.087	0.63	0.14
Fig. 3 (Kiang, 2002)	OAK	2.91	3.29	0.015	0.364	5.20	5.40		1.13	0.64
Fig. 3 (Barford et al., 2001)	HF	3.14	5.03	0.041	0.926	13.18	16.19		1.60	7.96

^a Tree geometry parameters, some of these parameters are illustrated in Fig. 1.

^b λ , stem count density in square meters.

^c F_a , foliage area volume density within a single crown.

^d γ_E , the needle-to-shoot-clumping factor = 1.48 for Fig. 12.

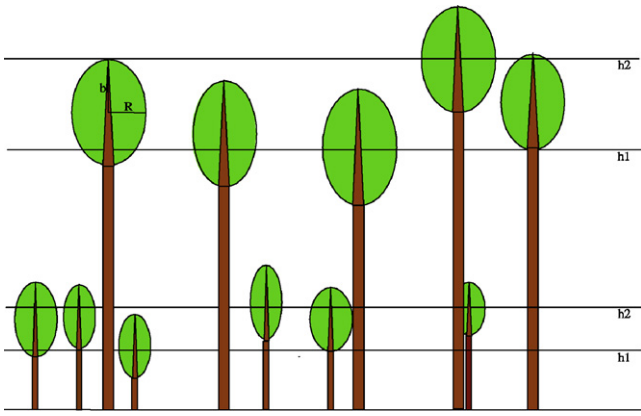


Fig. 1. Vertical cross-section of a two-layer vegetation canopy scene showing the tree crown with ellipsoid shape and different size and density distributed in space, as modeled in geometrical optical and radiative transfer (GORT). In this figure, vertical and horizontal crown radii are labeled as b and r , while the height of lower and upper-bounds of crown centers are labeled as h_1 and h_2 for both overstorey and understorey layers.

(PAR) transmission, solar radiation transmission, and absorption by canopy elements in conifer forests (Ni et al., 1997), bidirectional reflectance (Ni et al., 1999a; Ni and Li, 2000), surface albedo (Ni and Woodcock, 2000), and spatial variance of remotely sensed images over vegetated land surfaces (Ni et al., 1999b; Ni and Jupp, 2000). Song and Woodcock (2002), Song et al. (2002) and Song and Woodcock (2003) used the GORT model successfully to model the reflectance of Oregon forest stands as a function of age or successional stage as well as observed effects of topography and view angle on optical imagery.

Our strategy to simplify GORT is to account for vegetation vertical and horizontal heterogeneity in an analytical scheme. Vertically, foliage is not distributed evenly, with more leaf area in the middle than the top and bottom of the canopy (Wang et al., 1990). We account for the vertical foliage area profile by calculating the actual foliage profile using described tree geometry parameters such as tree size, density, foliage area volume density within a crown, and tree height distribution.

Horizontally, hierarchical clumping exists, with needle leaves on shoots, shoots and foliage on branches inside crowns, crowns in forest stands, and stands in landscapes. At the stand level, GORT assumes trees are randomly distributed in space. In nature, young canopies tend to have trees randomly distributed, and the process of self-thinning then leads to a uniform spatial distribution in mature canopies (Moeur, 1997). We developed an analytical expression for the clumping factor incorporating the assumption that crowns do not overlap, which describes a crown spatial distribution intermediate between completely random versus uniform. The clumping factor is an analytical function of crown geometry and tree density to account for the horizontal clumping effect, that is, the horizontal heterogeneity in vegetation structure. By incorporating the clumping factor, the uncollided direct beam transmittance or canopy gap probability by height, $P_{\text{gap}}(\theta, z)$ can be described as:

$$P_{\text{gap}}(\theta, z) = \exp\left(\frac{-\gamma(\theta)G(\theta)L(z)}{\cos(\theta)}\right) \quad (3)$$

where z is the height in the canopy, and $L(z)$ is the cumulative leaf area index from the canopy top to height z . The clumping factor, $\gamma(\theta)$, is a function of solar zenith angle and possibly height (full derivation provided in Section 2.1). The product of $\gamma(\theta)$ and $L(z)$ is the effective leaf area index, $L_e(z)$.

To model the vertical heterogeneity in vegetation canopy reflectance and transmittance and absorption in dynamic global vegetation models (DGVMs), we developed a coupled analyti-

cal GORT and two-stream scheme for our usage. The full model development including the analytical clumped leaf + stem/branch GORT, the effect of the trunk on light, and the coupled GORT and two-stream scheme will be described in this section. We call this complete scheme the analytical clumped two-stream (ACTS) model.

2.1. The analytical clumped-foliage GORT gap probability model

The portion of photons passing through the gaps within the vegetation canopy without hitting any canopy elements is defined as the canopy gap probability or uncollided transmittance. Canopy gap probability is the most important variable to describe the clumping effect on light interactions with plant canopies. For heterogeneous plant canopies, GORT calculates both the between-crowns and within-crowns gap probabilities separately based on geometric optical and radiative transfer theory. To simplify the full GORT model, we assume that the canopy gap probability follows an exponential decay, similar to Beer's Law used in pure radiative transfer theory for a homogeneous plant canopy. However we allow for both vertical and horizontal variations of foliage. We model the vertical variation of foliage using the method described in Ni-Meister et al. (2001). We characterize horizontal variation of foliage by a stand-scale clumping factor, for which an analytical expression based on canopy geometry is derived below. Although clumping can vary vertically, we justify the use of a stand-scale clumping factor in the development below.

2.1.1. Vertical foliage profile and justification of stand-scale clumping factor

The attenuation of radiation passing through a canopy is directly affected by the density, size, and distribution (horizontal and vertical) of foliage and woody elements within the canopy, as well as spectral properties of leaves, woody elements, and the surface albedo beneath the canopy. We take the same assumption of the full GORT model that ellipsoidal tree crowns are vertically randomly distributed in three-dimensional space with mean horizontal and vertical crown radii r and b , respectively; foliage area volume density, F_a (leaf area per crown volume, m^2/m^3); tree density λ (number per area, m^{-2}); and the heights h_1 and h_2 , defined as mean crown center height minus and plus two times its standard deviation, respectively (see Fig. 1) for the scene of GORT). The statistical projected foliage area density profile, (defined as leaf area index per vertical unit) at height z , $dL(z)/dz$ (m^{-1}), is calculated for the following two cases as described in Ni-Meister et al., 2001 (see Appendix A for details):

Fig. 2 shows the statistical foliage area density for canopies with identical tree heights and an example with random tree heights. For both single-height and random-height canopies, larger foliage area concentrates in the middle part of the canopy, with greater spread for the varying-height canopy. The tree geometry parameters (listed in Table 1) are from a deciduous forest in Morgan-Monroe State Forest (MMSF), Indiana (Yang et al., 2010). Table 1 lists all the input parameters for all simulations presented in this study.

To check the effectiveness of the statistical foliage density profile in capturing the gap probability, we compared canopy gap probability profiles in actual stands calculated from the full GORT model, a layered Beer's law (without clumping), and a layered Beer's law with a clumping factor. The latter two cases are different from the traditional Beer's law in that they allow for vertical variation of foliage, which is calculated based on the formula presented above.

The clumping factor for the observed stands was calculated through a fitting method. First, we calculated the canopy gap fraction vertical profile using the full GORT model, and then we fit the layered, clumped Beer's law to this profile. We obtained the fitted

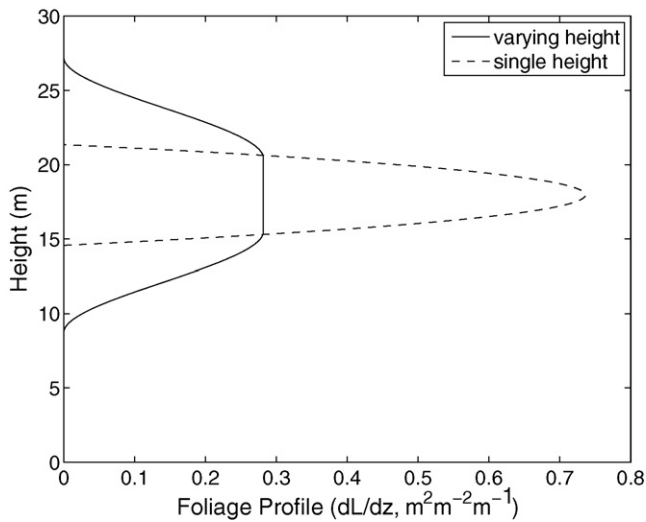


Fig. 2. Comparison of foliage profile for canopies with single-height trees and varying-height with the same canopy geometry parameters. The total leaf area index is 3.30.

clumping factor values by solving for $\gamma(\theta)$ from Eq. (1), fitting to canopy gap fraction, $P_{\text{gap,GORT}}(\theta,z)$ at the bottom of the canopy as calculated by the full GORT model:

$$\gamma(\theta) = -\frac{\cos \theta \cdot \ln(P_{\text{gap,GORT}}(\theta, 0))}{G(\theta)L_t} \quad (4)$$

where $P_{\text{gap,GORT}}(\theta,0)$ is the gap fraction modeled by the full GORT at solar zenith angle θ and at the bottom of the canopy.

Fig. 3 shows that the layered, clumped Beer’s law fits well the full GORT model prediction for an oak-savanna site for a sparse canopy example (Kiang, 2002), and a temperate broadleaf forest in Harvard Forest, Massachusetts for more closed canopy example (Barford et al., 2001) (see Table 1 for the inputs). The gap fraction from both the clumped and layered Beer’s Law shows a sigmoid shape of the profile. Layered Beer’s Law describes the canopy gap probability as an exponential decay with cumulative LAI. However, the vertical LAI profile is not uniform and is calculated from Eq. (5).

Fig. 3 shows that using the statistical mean canopy foliage profile accounts well for the vertical variation of light transmission.

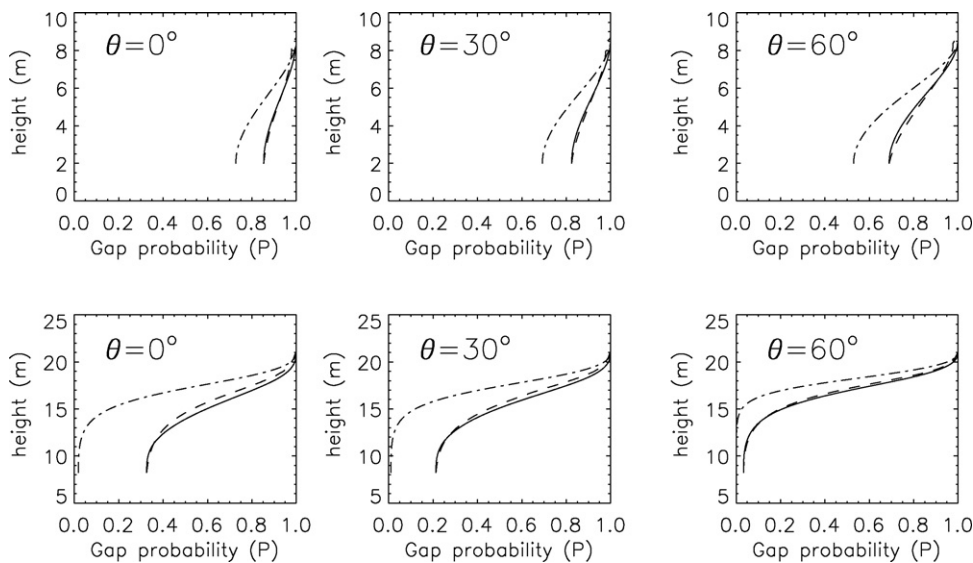


Fig. 3. Comparison of canopy gap probability at three solar zenith angles (0° , 30° and 60°) between the full GORT model (solid line), layered Beer’s law (dot-dashed line) and clumped Beer’s law (dashed line) in an oak-savanna in CA (top three panels) and a deciduous forest in the New England region (bottom three panels).

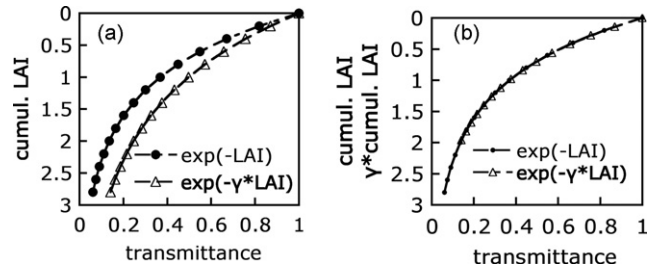


Fig. 4. Distinction between plotting transmittance against (a) actual LAI versus (b) model effective LAI (example has $\gamma = 0.7$).

It also demonstrates that a constant clumping factor through the vertical canopy profile very closely predicts the entire vertical light profile. Therefore, although, strictly speaking, the clumping factor may vary by height in the canopy, we can achieve a parsimonious model by simplifying the problem by solving for the clumping factor merely from the gap probability at the bottom of the canopy. This effectively integrates the transmission of light through the entire canopy.

Note that plotting the light transmission versus height is equivalent to plotting against actual LAI profiles, since at each height in the canopy, all models must transmit through the same actual LAI. All the models compared here will calculate different effective LAI due to different representation of clumping. If their transmittance is plotted against the effective LAI as seen by each respective model, then of course all of their transmittance curves will fall on the same line. Using as examples a simple Beer’s Law versus a clumped Beer’s Law equation, Fig. 4 illustrates how the difference in transmittance, is easily visualized when plotting against (a) actual LAI, while if (b) the effective LAI (actual LAI for Beer’s Law, effective LAI equal to $\gamma \times$ LAI for the clumped Beer’s Law), then the transmittance curves must fall on top of each other. Since plotting against effective LAI does not illustrate well the difference in performance of the models, and since we will eventually be comparing the models to height-based field measurements of transmittance, we plot model results from here on against height within the canopy, which is equivalent to plotting against actual LAI in comparing model performance.

In Section 2.1.2 we now derive an analytical, prognostic expression for the clumping factor at the bottom of canopies.

2.1.2. Analytical formula for crown clumping factor, γ

The above analysis clearly shows that the canopy gap fraction or uncollided direct beam transmittance profile modeled by full GORT model can be approximated by an exponential decay with the vertical variation of foliage and with a foliage clumping factor. We now derive an analytical formula for the clumping factor from the GORT model, but with one additional constraint that improves the realism in the analytical model. The assumption of the full GORT model is that the tree crown centers are randomly distributed in space. With this assumption, tree crowns can overlap. For the analytical clumping factor, we assume that tree crown centers are still randomly distributed in space with the constraint that they do not overlap. This assumption for the analytical GORT is closer to what is found in nature, since trees grow to avoid overlap of crowns, and mature canopies will tend toward a more regular horizontal spatial distribution (Kenkel, 1988). The full GORT is biased toward more clumping relative to nature. As mentioned earlier, in a subsequent validation paper we compare the analytical model with ground data rather than with the full GORT model simulation alone as the full GORT is still just a model, but it is useful for theoretical study in this paper.

For the analytical expression of the Beer's law clumping factor in Eqs. (1) and (3), we slightly modified the results from Li and Strahler (1988) (see Appendix B for details) to obtain the clumping factor as,

$$\gamma = \frac{3}{4\tau_0 r} \left(1 - \frac{1 - (2\tau_0 r + 1)e^{-2\tau_0 r}}{2\tau_0^2 r^2} \right) \quad (5)$$

where $\tau_0 r = 3GL_t/4\lambda\pi \cdot r^2$ for spherical crowns.

The above equation is an exact formula and is slightly different from what was presented as an approximation in Li and Strahler (1988). The above formula only works when crowns are spheres. To extend the sphere crowns to more general ellipsoid crowns, Li and Strahler (1988) introduced a linear transformation factor

$$\Gamma = \frac{\cos \theta}{\cos \theta'} = \left(\frac{1 + (b/r)^2 \tan^2 \theta}{1 + \tan^2 \theta} \right)^{1/2}, \quad (6)$$

where θ and θ' are solar zenith angle in ellipsoid and sphere spaces respectively (see Fig. 5 for their relationship). The transformation factor represents the ratio of crown projected area in spherical space to the ellipsoid space, so for ellipsoid crowns (see Fig. 5 for

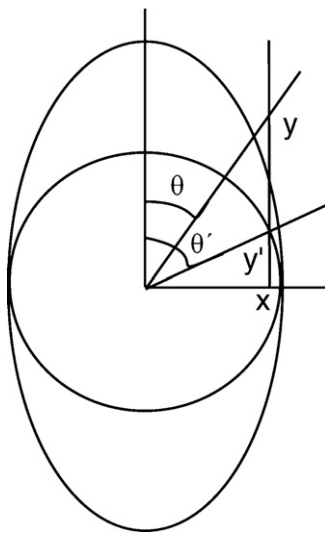


Fig. 5. Linear transformation from sphere space to ellipsoid space. θ and θ' are solar zenith angles in ellipsoid and sphere space respectively. $\tan \theta' = (b/r)\tan \theta$ and $\Gamma = \cos \theta / \cos \theta' = \sqrt{1 + ((b/r)\tan \theta)^2 / 1 + \tan^2 \theta}$.

the detailed transformation), $\tau_0 r$ in Eq. (12) becomes,

$$\tau_0 r = \frac{3GL_t}{4\lambda\pi \cdot r^2 \Gamma} = GF_{ar} \left(\frac{1 + \tan^2 \theta}{1 + (b/r)^2 \tan^2 \theta} \right)^{1/2}. \quad (7)$$

Thus, γ depends on incident zenith angle θ . The clumping factor accounts for not only direct beam, but also diffuse radiation. The diffuse clumping factor is calculated by integrating clumping factors for all possible incident zenith angles.

Fig. 6 shows the sensitivity of the clumping factor to tree density, crown size (horizontal crown radius), foliage area volume density, and crown shape (ratio of vertical and horizontal crown radii) calculated by both the analytical and full GORT model for 32 deciduous plots in Harvard Forest, MA (Barford et al., 2001). Only tree height and diameter at breast height (DBH) are measured, while the rest of GORT input parameters are calculated based on allometric equations (Pacala et al., 2001; Albani et al., 2006). The change in the clumping factor with different structure parameters shows very similar patterns for the analytical and full GORT models. The clumping factor increases with tree density, crown shape (when ratio of vertical and horizontal crown radii is greater than 1), indicating that a canopy is more homogeneous with increasing tree density and b/r ratio. The clumping factor decreases with crown size and foliage area volume density, indicating that the canopy is more clumped with the increase of crown size and foliage area volume density. One exception is that the clumping factor estimated by the full GORT is close to constant at a solar zenith angle of 0° .

To analyze the difference in clumping factors estimated by the analytical and full GORT models, Fig. 7 compares the two models for the same forests as used in Fig. 6. The analytical clumping factor is larger than the full GORT modeled values, because the full GORT assumption of random crown distributions results in over-clumping. The analytical clumping factor is always larger – less clumped – since it takes into account the condition that tree crowns do not overlap. The difference becomes smaller at larger solar zenith angles. In a companion paper, Yang et al. (2010) fully evaluate the relative accuracy of these two clumping factors by comparing the light profiles modeled using these two factors with ground measurements in several different forest types.

2.1.3. Needle-to-shoot-clumping factor, γ'

Compared to broadleaf forests, coniferous forests have additional needle-to-shoot level clumping, which enhances clumping and its effect on radiative transfer. In some previous models of needle-to-shoot-clumping, shoots are treated as the basic structure elements for modeling canopy light interception and photosynthesis (Oker-Blom et al., 1983, 1991), and the shoot level structure and scattering properties are used to derive the canopy radiative transfer scheme.

The clumping is also often modeled as two components for conifer forests: clumping at scales larger than the shoot (crown and branch level from Eq. (5)) and within shoots. The needle-to-shoot level clumping is quantified using the needle-to-shoot area ratio, γ_E , which is measured through shoot samples and varies from species to species, ranging from 1.05 to 1.86 (Chen, 1996) or the shoot silhouette to total area ratio (STAR) (Oker-Blom and Smolander, 1988). STAR acts as the G-function (leave orientation) defined for flat leaves, but also takes into account the clumping effect due to mutual shadowing of needles in the shoot, which decreases the single scattering of shoots. The hemispherically averaged STAR or \overline{STAR} is equal to $1/4\gamma_E$. The shoot level clumping index is used to derive shoot level structure and scattering properties (Lang, 1991).

Following the approach by Chen (1996), we calculate the shoot level LAI as needleleaf area index divided by the needle-to-shoot

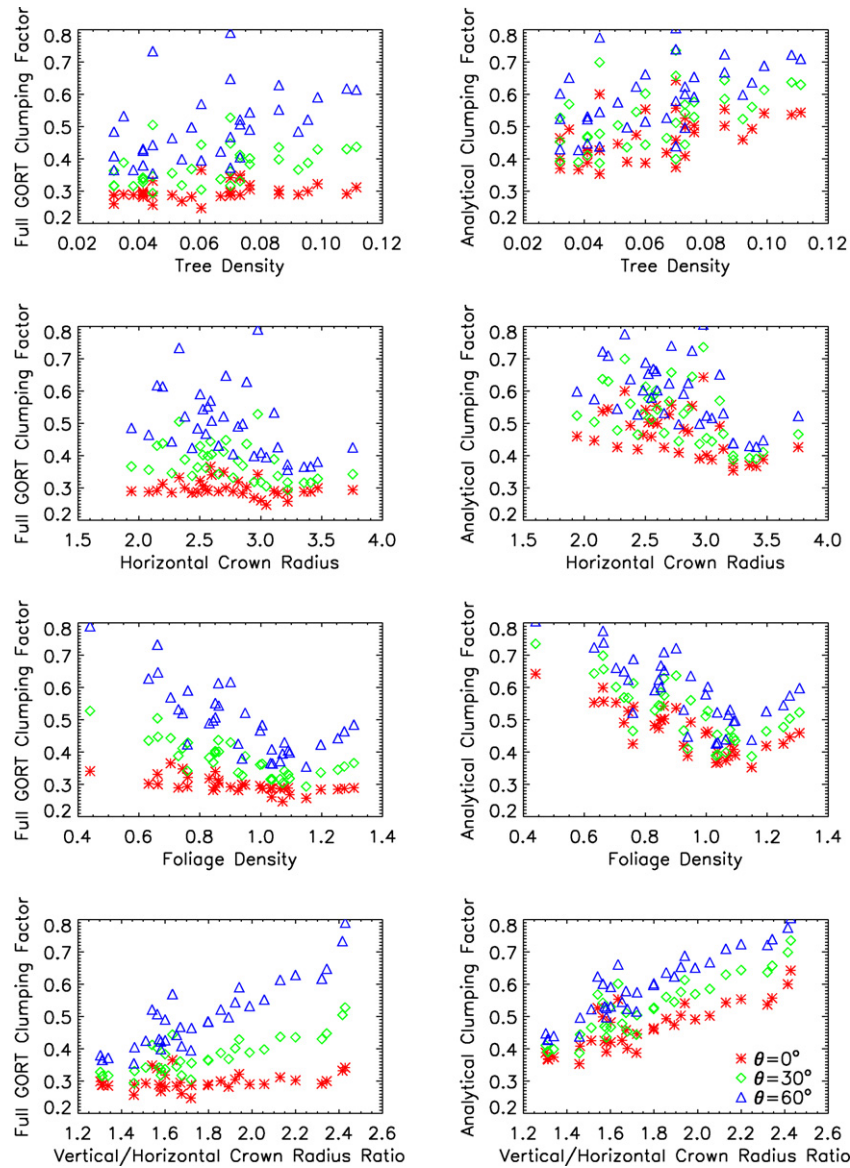


Fig. 6. Change of clumping factor as a function of tree density, horizontal crown radius, foliage density and vertical/horizontal crown radius ratio for the full (left panels) and analytical (right panels) GORT models.

area ratio, γ_E

$$L_{sh} = \frac{L_n}{\gamma_E} \tag{8}$$

This approach is equivalent to the clumping factor for conifer forest, γ' , modeled as:

$$\gamma' = \frac{\gamma}{\gamma_E} \tag{9}$$

in which γ has the expression of Eq. (12). The shoot level scattering properties will be presented in Section 2.3.

2.1.4. Clumped-foliage GORT model for multilayered vegetation canopies

The above scheme only works for a single-story vegetation canopy. However multi-story and multispecies vegetation canopies commonly exist, e.g., deciduous trees as overstory, and late succession trees, shrubs or grasses as understory. Leaf orientation, foliage density within crowns, crown shape, size and density are different at different layers, thus the G-function and clumping factor are different. In this case, $P_{gap}(z, \theta)$ is calculated through convolution of

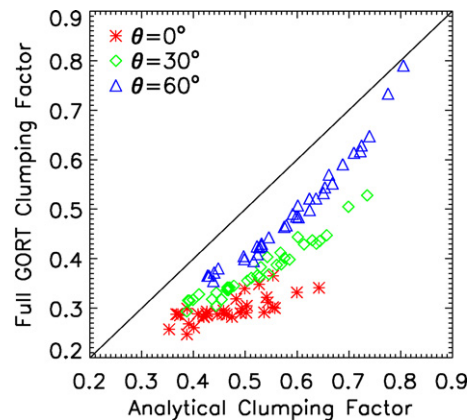


Fig. 7. Comparison of clumping factors calculated from the full GORT and analytical GORT models.

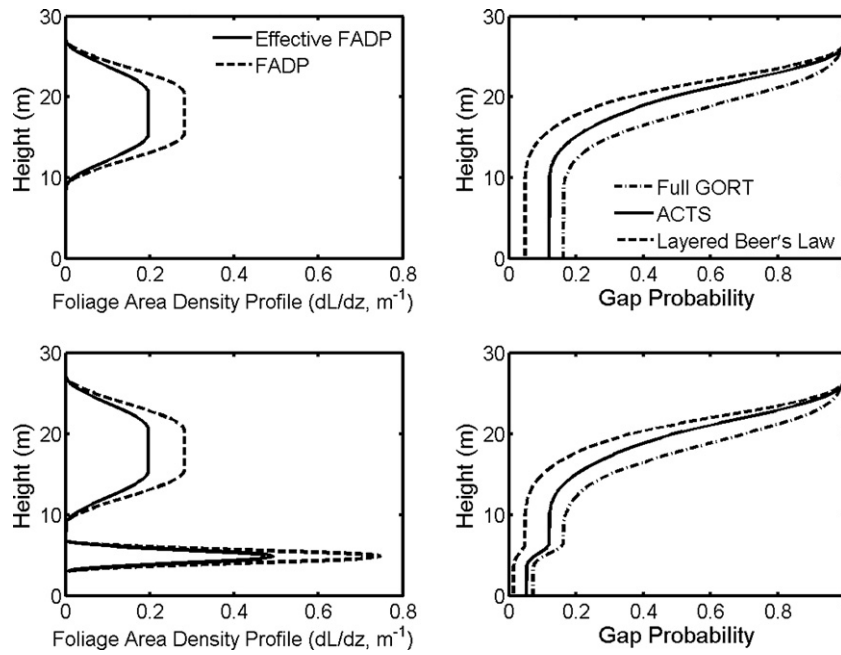


Fig. 8. Comparison of (a) clumped and non-clumped effective foliage density, L_e , profile and (b) gap probability at solar zenith angle 60° . Profiles in (c) and (d) are similar to (a) and (b), but for a two-story canopy.

the effective projected leaf area index, that is:

$$P_{\text{gap}}(z, \theta) = \exp\left(\frac{-L_e(z)}{\cos \theta}\right)$$

$$L_e(z) = \int_z^{(h_2+b)_{\text{max}}} \sum_i L_{ei}(z) dz \quad (10)$$

$$L_{ei}(z) = \gamma_i(\theta) G_i(\theta) L_i(z)$$

where i is plant functional type or class, $\gamma_i(\theta)$ is the clumping factor for class i , $G_i(\theta)$ is the leaf orientation factor for layer i , and $L_i(z)$ is the cumulative leaf area at height z for class i .

Fig. 8 shows the comparison of statistical mean foliage area density profiles and gap fraction at solar zenith angle 60° between clumped and non-clumped models for a one-layer and a two-story canopy in a deciduous forest in Morgan-Monroe State Forest (MMSF), Indiana (see Table 1 for inputs). For comparison, the gap fraction from the full GORT model is also shown. The clumping factor is 0.70 for the overstory and 0.66 for the understory for the one-layer (overstory only) and two-layer canopies, respectively. There is no overlapping between overstory and understory for the two-layer canopy. Fig. 8 shows that the effective foliage profile from clumping is reduced compared to the non-clumped vegetation canopy, resulting in a larger gap fraction for the clumped canopy than the non-clumped one. The gap probability is enhanced by the clumping factor, especially at the bottom of the canopy; the enhancement could be more than 100%, which is significant for the subsequent canopy transmittance, absorbance and snow melting. Since crowns can overlap in the full GORT but not in the analytical model, the full GORT model results show comparable but slightly larger gap fractions compared to the analytical clumped model results. In summary, the gap fraction modeled by both the full GORT model and the analytical clumped model is larger than the model results by the layered but non-clumped model, indicating ignoring clumping can lead to underestimation of the gap fraction.

2.2. The analytical clumped leaf + branch + trunk GORT model

Gap fraction and light transmission within a vegetation canopy are also affected by trunks and stems/branches. The effect on light

transmission can be particularly large during the leafless or leaf-off season, and correctly modeling this effect on light transmission is crucial for correctly predicting ground temperatures and the snowmelt rate. The effect of trunks on below-canopy lidar laser pulse interaction with the vegetation canopy has been implemented in the full GORT model (Ni-Meister et al., 2008). A similar approach is implemented in this analytical GORT model to take into account the effect of trunks and stems/branches.

To account for the effect of branches on gap probability, we modified the foliage area volume density F_a as a plant area volume density, P_a , which incorporates both branches and foliage, exclusive of the trunk. The G -function for branches is like that of the leaves due to self-similarity (West et al., 1999; Enquist and Niklas, 2001). To account for the effect of trunks on gap probability, we modeled the between-trunk gap probability, $P_{\text{trk}}(z, \theta)$ as an exponential decay function of the projected trunk area, $S_{\text{trk}}(z, \theta)$, based on Boolean set theory (Ni-Meister et al., 2008), following the same approach used to calculate the between-crown gap probability as in Li et al. (1995) and Ni et al. (1997):

$$P_{\text{trk}}(z, \theta) = \exp(-\lambda S_{\text{trk}}(z, \theta)) \quad (11)$$

where λ is the crown county density and $S_{\text{trk}}(z, \theta)$ is the mean projected trunk area at height z and is calculated as a function of trunk diameter at breast height (DBH), tree height, and incident zenith angles.

$S_{\text{trk}}(z, \theta)$ is calculated for two types of tree growth forms: one for broadleaf forests or rounded crowns, and one for coniferous forests or conical crowns. For rounded crowns, the trunk is treated as a cylinder from ground to the crown center following Ni-Meister et al. (2008):

$$S_{\text{trk}}(z, \theta) = \frac{DBH}{h_2 - h_1} \cdot \tan \theta \cdot \int_{h_1}^{h_2} \max((z' - z), 0) \cdot dz' \quad (12a)$$

For a uniform canopy, $h_1 = h_2$,

$$S_{\text{trk}}(z, \theta) = DBH \cdot \tan \theta \cdot \max((h_2 - z), 0). \quad (12b)$$

For coniferous forests or conical crowns, the trunk is modeled as a cylinder below crowns and as a cone within crowns, following

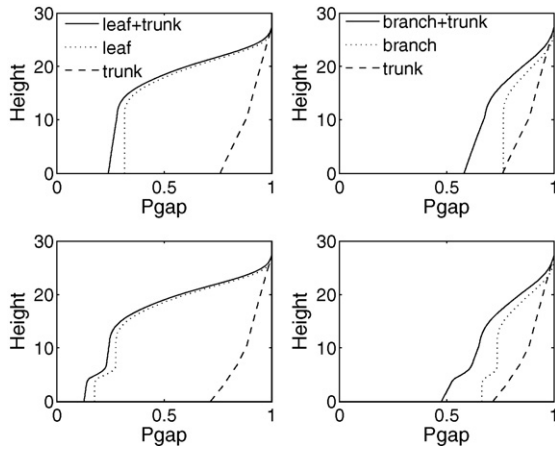


Fig. 9. Comparison of gap probability with regarding to trunk effect for (a) one story leaf-on canopy, (b) one-story leaf-off canopy, (c) and (d) are their two-story counterparts at solar zenith angle 45°.

Nilson and Kuusk (2004):

$$S_{\text{trk}}(z, \theta) = \frac{1}{2} \cdot \frac{DBH}{h_2 - h_1} \cdot \tan \theta \cdot \int_{h_1}^{h_2} (z' + b + \frac{h_2 - h_1}{2} - z) \cdot dz', \quad z > h_1 - b \quad (13a)$$

$$S_{\text{trk}}(z, \theta) = \frac{DBH}{h_2 - h_1} \cdot \tan \theta \cdot \int_{h_1}^{h_2} (z' - z) \cdot dz', \quad z \leq h_1 - b. \quad (13b)$$

For a uniform canopy, $h_1 = h_2$,

$$S_{\text{trk}}(z, \theta) = DBH \cdot \tan \theta \cdot (h_2 + b - z), \quad z > h_1 - b \quad (13c)$$

$$S_{\text{trk}}(z, \theta) = DBH \cdot \tan \theta \cdot (h_1 - z), \quad z \leq h_1 - b \quad (13d)$$

Then the total gap probability is a function of the between-trunk gap probability and leaf + branch gap probability,

$$P_{\text{gap}}(\theta) = \exp \left(- \left(\frac{GL\gamma}{\cos \theta} \right) + \lambda S_{\text{trk}} \right) \quad (14)$$

The only difference is within the crown: for the rounded crown scheme, there is no trunk above the crown center, and thus the trunk effect on gaps is none. For the conical crown scheme, the trunk radius linearly decreases with increasing height. However, these two schemes produce the same trunk gap probabilities below crowns due to the tapering of the trunk above.

Fig. 9 shows the gap probability profiles at a solar zenith angle of 45° calculated with trunks only, leaves only, and leaves plus trunks, for the cases of leaf-on (left column) and leaf-off (right column), and for a single-story canopy (top row) and a two-story canopy (bottom row). Parameters are taken from a broadleaf deciduous forest in Morgan-Monroe State Forest (MMSF), Indiana (Table 1 for the inputs). The trunk-only and foliage-only gap probabilities show distinct vertical profiles: leaf-only probabilities show a sigmoid shape with decreasing height, characterized by a sharp decrease in the upper canopy, a slow decrease in the lower canopy, and constant values below the crowns. However the trunk-only gap probabilities show a piecewise linear trend with decreasing height: a slow decrease within the crowns, and a faster decrease below crowns.

The impact of trunks on total gap probability is stronger during the leaf-off than the leaf-on season for both one-story and two-story canopies. For the leaf-on cases, in Fig. 9a and c, though the gap fraction with only trunks can reach 0.77 at the bottom of canopy, the contribution of the trunk effect when both leaves and trunks are included is less than 0.07. In general, in fully leaved canopies or at the solar zenith angle of zero degrees, the trunk effect

becomes insignificant. However, for the leaf-off cases (Fig. 9b and d), although having differing profiles, at the bottom of the canopy the trunk-only and branch-only gap fractions are comparable. Both contributions are too significant to be neglected. Thus, in a deciduous broadleaf forest for the leaf-off season, the canopy still blocks the penetration of light.

We note that the impact of the leafless canopy is not only with regard to the decay pattern of the transmittance profile, but also on the spectral aspect of the radiation balance, which affects the momentum, heat and energy transfer patterns within the canopy and the boundary layer. These issues will be quantified in a later paper that couples the canopy radiative transfer model to a vegetation and land surface model.

2.3. The clumped two-stream scheme

Having obtained improved gap probabilities with the analytically derived clumping factor and the trunk effect depicted in Section 2.2, we can now get unscattered direct beam transmittance, and diffuse transmittance by some more modifications. Total transmittance (unscattered and scattered) is required for estimating solar and thermal radiation at the snow surface underneath the canopy in addition to the absorbed and reflected radiation for vegetation and atmospheric coupling. To meet these needs, we introduce the two-stream scheme.

2.3.1. Model modification

The two-stream scheme is used to model radiative transfer in plant canopies, with the assumption that the scattering in the canopy is isotropic. The original two-stream scheme, which accounts only for a single-layered homogeneous plant canopy, is currently used in major land models, such as BATS (Dickinson, 1983; Dickinson et al., 1986) and CLM (Bonan et al., 2002). Here, we modify it to suit multilayered heterogeneous plant canopies by introducing (i) multilayered foliage profiles instead of a single leaf area index value, and (ii) the clumping factor. The two-stream equations in Dickinson (1983), Sellers (1985), and Sellers et al. (1996) are rewritten as:

$$\begin{aligned} \bar{\mu} \frac{dI^\uparrow(L')}{dL'} + [(1 - (1 - \beta)\omega)I^\uparrow(L') - \omega\beta I^\downarrow(L')] &= \omega \bar{\mu} \kappa \beta_0 \exp(-\kappa L') \\ \bar{\mu} \frac{dI^\downarrow(L')}{dL'} + [(1 - (1 - \beta)\omega)I^\downarrow(L') - \omega\beta I^\uparrow(L')] &= \omega \bar{\mu} \kappa (1 - \beta_0) \exp(-\kappa L') \end{aligned} \quad (15)$$

where $L' = \gamma L$, and corresponding modifications are applied to the solutions. In considering multilayered heterogeneous plant canopies, different layers of the canopy could have different G -functions. We propose an iterative method with the simple idea to preserve the total extinction item in (1). For a two-layered case with original LAI of L_1 and L_2 , clumping factors $\gamma_{1,0}$ and $\gamma_{2,0}$, and G -functions $G_{1,0}$ and $G_{2,0}$, the calculation is expressed as

$$G_{k+1} = \frac{\gamma_{1,0} G_{1,0} L_1 + \gamma_{2,0} G_{2,0} L_2}{\gamma_{1,k} L_1 + \gamma_{2,k} L_2} \quad (16)$$

$$\gamma_{1,k+1} = \gamma_1(G_{k+1})$$

$$\gamma_{2,k+1} = \gamma_2(G_{k+1})$$

where $k = 0, 1, 2, \dots$; G_k is the k -th iteration of average G -function, $\gamma_{1,k}$ and $\gamma_{2,k}$ are k -th iteration values of clumping factors for two layers, and γ_1, γ_2 are functions as Eq. (12). In the calculation, the values converge quickly. Generally, the relative error of G is within 3% by the first iteration. This result is important to know, because it will be necessary to limit the number of iterations and hence computational cost in using this scheme in a DGVM in a land surface model

when coupling to an atmospheric GCM. In a future paper describing the implementation of this canopy radiative transfer scheme in the Ent DGVM, we will demonstrate that one iteration is sufficient.

For the case of conifer forests, we substitute ω , the leaf scattering coefficient, with ω_{sh} , a shoot scattering coefficient that treats shoots with needles on them as the basic scattering element. The scattering property (single scattering albedo) of shoots is calculated from single scattering albedo of needles and needle-to-shoot level clumping based on spectral invariant theory (Knyazikhin et al., 1998; Smolander and Stenberg, 2003) as:

$$\omega_{sh} = \omega_N \frac{4\overline{STAR}}{1 - \omega_N(1 - 4\overline{STAR})} = \omega_N \frac{1}{\gamma_E - \omega_N(\gamma_E - 1)} \quad (17)$$

where ω_{sh} and ω_N are the single scattering albedo of shoot and needle respectively, and γ_E is the needle-to-shooting area ratio and directly related to the hemispherically averaged silhouette to total area ratio $\overline{STAR} = 1/4\gamma_E$ (Rochdi et al., 2006; Lang, 1991). Shoot level scattering properties, ω_{sh} , and structure inputs L_{sh} calculated by Eq. (8) will be used to drive the clumped two-stream model for conifer forests.

2.3.2. Canopy absorption, reflection, and transmission

The fractions of sunlit vs. shaded leaves are important to distinguish, because sunlit leaves will receive a much higher light flux density than shaded leaves under sunny conditions, such that their photosynthetic rates will be significantly different (Spitters, 1986; Baldocchi and Collineau, 1994; Wang and Leuning, 1998; Leuning et al., 1998). This partitioning is also necessary for accurate prediction of canopy radiation absorption. Shaded leaves receive diffuse light only, while sunlit leaves receive both diffuse and direct radiation. The derivation of the fractions and related absorption is provided in Dai et al. (2004) and Wang (2003), as

$$A_{sha}(L') = \sum_{j=b,d} I_j(1 - \omega)(I_j^\uparrow(L') + I_j^\downarrow(L'))$$

$$A_{sun}(L') = (1 - \omega)\kappa I_b + A_{sha}(L') \quad (18)$$

$$A_{tot}(L') = \int_0^L A_{sun}(L')f_{sl}(L') + A_{sha}(L')f_{sha}(L')dL'$$

Note that first two equations in (18) describe radiation absorbed per unit leaf area, accounting only for a single layer in the foliage profile, while the third equation in (18) accounts for leaf area of the whole canopy. The sunlit leaf fraction, f_{sl} , is calculated similarly to the gap probability expression in Eq. (1), and the shaded fraction, f_{sha} , is simply one minus the sunlit fraction.

Assuming that there is no light source from the background, reflected light comes from two components of upward radiation: (i) upward diffuse radiation caused by direct beam incident, and (ii) upward diffuse radiation caused by diffuse light incident, and the equation is simply:

$$R(L') = I_b \cdot I_b^\uparrow(L') + I_d \cdot I_d^\uparrow(L'). \quad (19)$$

Note that (B4) is a special case of (19).

The processing of transmission is similar to that of absorption. We need to consider three components of downward radiation: (i) gap probability, the direct beam penetration fraction without interaction with canopy elements; (ii) downward diffuse radiation caused by direct beam incident; and (iii) downward diffuse radiation caused by diffuse light incident. Transmission for a single layer can be written as:

$$T(L') = I_b \cdot \frac{\exp(-GL')}{\cos \theta + I_b^\uparrow(L')} + I_d \cdot I_d^\downarrow(L') \quad (20)$$

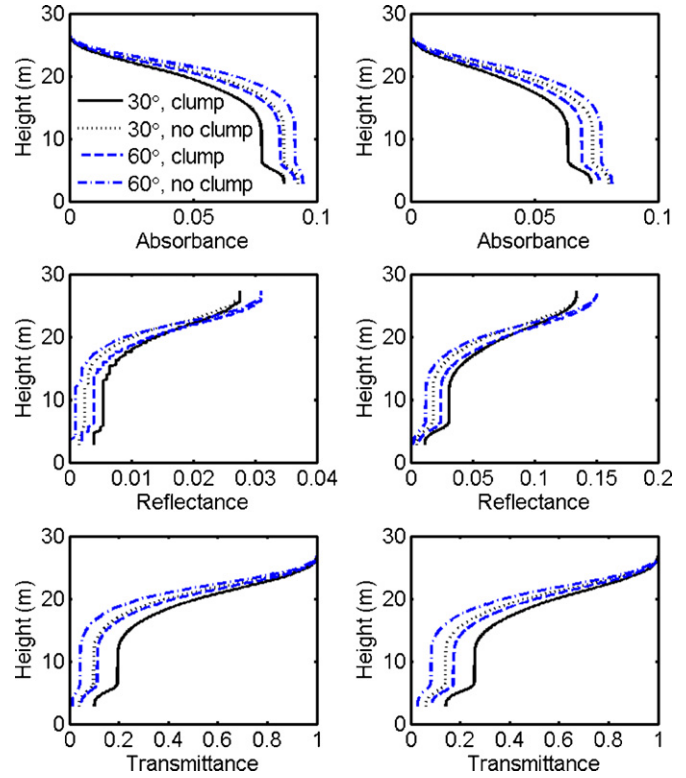


Fig. 10. Normalized absorbance, reflectance and transmittance profile for visual band (left panels) and near-infrared band (right panels) at 30° and 60° solar zenith angle. Note the scale for visual and near-infrared band of reflectance is not the same.

And the following conservation law holds true by introducing background albedo, ρ_s :

$$A_{tot}(L_t) + R(0) + (1 - \rho_s)T(L_t) = 1. \quad (21)$$

3. Results

The previous sections have presented our analytical derivation of the foliage clumping factor, shoot-clumping factor, trunk effect on scattering, and two-stream multilayered, sunlit/shaded leaf, canopy radiative transfer scheme. We call this suite of model components the analytical clumped two-stream (ACTS) canopy radiative transfer model. With the complete ACTS, we examine finally the profiles of canopy absorption, reflection and transmission, and their sensitivity to some factors such as solar zenith angle, background and density of the canopy, comparing particularly the clumped and non-clumped models.

3.1. Clumping effect on vertical profiles

Fig. 10 displays absorption, reflection, and transmission profiles for visible and near-infrared wavelengths for the same two-story canopy as in Fig. 8 (see Table 1 for inputs), at 30° and 60° incident zenith angles, and the direct beam ratio is set to 0.5. Generally, the absorption profiles resemble foliage profiles, which could be interpreted as more leaf exposure in the light leading to more canopy absorption for both visible and near-infrared wavelengths. Visible radiation shows relatively larger absorption. The upper part of the upper story canopy receives most of the direct beam, and the direct beam can penetrate to deeper level due to hierarchical clumping. The heights of absorption peak and foliage density peak shift between the two models. In the $\theta = 60^\circ$ case, for example, the absorption profile reaches a maximum at 21.8 and 21.1 m for non-clumped and clumped models, respectively, while the foliage

profile reaches a maximum at 18.7 m. Also due to clumping, a higher portion of radiation is transmitted to the lower canopy. For a non-clumped model, the ratio of understory absorption maximum to upper story absorption maximum is 0.53, but the ratio for the clumped model with the same incident zenith angle is 0.63. For reference, the ratio of foliage maximum between the understory and upper story for both non-clumped and clumped models is 1.82, which demonstrates that as the sunlit leaf fraction decreases exponentially with canopy depth, the absorption by unit leaf area also decreases.

Due to clumping, the reflectance from the background is high at the bottom of the canopy, but the augmentation by foliage reflectance is low, and thus the reflectance at the top of the canopy is similar for both non-clumped and clumped models in this scenario. Reflectance from visible and near-infrared ranges at the bottom of the canopy is mostly from the background. Visible and near-infrared reflectance differences in the upper canopy increase with increased contribution from the canopy.

Transmittance profiles are similar to but larger than gap fractions due to the contribution from multiple scattering. Larger near-infrared transmittance than visible indicates that larger scatter transmittance contributes to the total due to more scattering in the near-infrared.

Another feature shown in Fig. 10 is that, with the introduction of the clumping factor, the radiation transmitted to the bottom of the canopy increases, and the canopy absorbance decreases, regardless of the incident zenith angle, or fraction of incident sunlit beam. For the $\theta = 30^\circ$ cases, as the sunlit fraction of the incident radiation increases, the canopy absorbance decreases and transmittance increases, which shows there is a higher absorption of diffuse light by a plant canopy than direct light. Due to the tradeoff between absorbance and transmittance with a dark soil as shown in this sample, the reflectance always stays the same for clumped and non-clumped models, but it does show variation with the direct beam ratio and solar zenith angle.

3.2. Dependence of clumping effect on solar zenith angle, total leaf area

To investigate the clumping effect dependence on solar zenith angles, vegetation density and background albedo, Fig. 11 provides a comparison of canopy total absorbance, top-of-canopy reflectance/total albedo and below-canopy transmittance change with solar zenith angles over the whole solar spectrum for sparse and dense canopies with dark/soil and bright/snow background for Morgan-Monroe State Forest (MMSF), Indiana. (See Table 1 for canopy structure inputs and Table 2 for soil and snow spectral inputs). Here, three spectral broad bands are used: visual (VIS, 0.3–0.74 μm), near-infrared (NIR, 0.74–1.35 μm), and mid-infrared (MIR, 1.35–4.0 μm), similar to Ni and Woodcock (2000). The radiation properties are calculated for each band, and then summed up with the weights derived from the solar spectrum (see Ni et al., 1997), so that for a quantity A , which can be absorbance, reflectance, transmittance, or albedo:

$$A = 0.50A_{\text{VIS}} + 0.35A_{\text{NIR}} + 0.15A_{\text{MIR}}. \quad (22)$$

Fig. 11 exhibits three expected patterns: (i) clumping in a canopy decreases absorbance, increases transmittance, but has little effect on reflectance for dense and sparse canopies with dark/soil background, while it leads to larger reflectance with a snow background. (ii) A denser canopy increases absorbance, decreases transmittance, but again has no effect on canopy reflectance with a dark soil background, but has a stronger effect on canopy reflectance with a bright snow background. For a canopy with a dark background, canopy reflectance is insensitive to the clumping factor and LAI, because the canopy reflectance saturates at a low LAI value, which

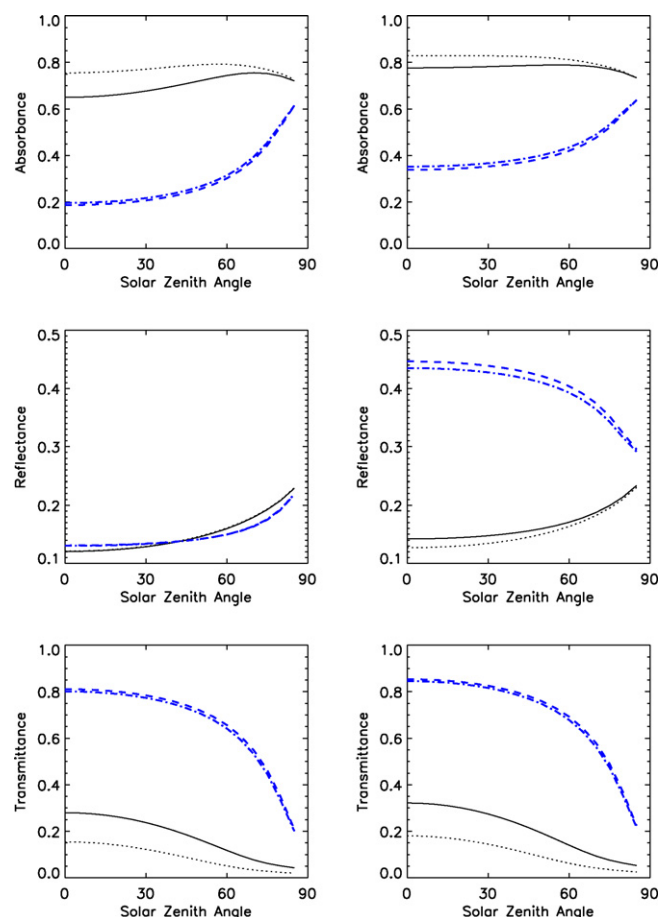


Fig. 11. Comparison of accumulated absorbance, reflectance and transmittance in the clear conditions for a broadleaf canopy with the background as soil (left panels) and snow (right panels).

is a limitation of the two-stream scheme. A sparser canopy leads to decreased absorbance, increased transmittance and increased canopy reflectance, particularly with bright snow background. For both dense and sparse canopies with a dark background, there is very little difference in reflectance values for clumped and non-clumped canopies. (iii) The clumping effect is more distinct in a denser canopy, and more sensitive to solar zenith angle. It is interesting to see that at a very high incident zenith angle, i.e. cases with θ greater than 80° , the absorbance for a dense canopy decreases. This can be interpreted as some portion of radiation escaping out of the canopy before it reaches the bottom with rather large zenith angles, and the larger the angle, the more portion of escaped radiation.

Fig. 12 shows the impact of needle-to-shoot-clumping on absorption, reflectance and transmittance in visible and near-infrared spectrum as a function of solar zenith angle for a conifer forest with the same crown structure inputs as in Fig. 8. We used the averaged needle structure input ($\gamma_E = 1.48$) from Chen (1996) and the spectral properties of needles from Sellers et al. (1996). In the visible range with little multiple scattering, using shoots as the basic element reduces effective LAI and thus also absorption, and increases total transmittance. Albedo shows no changes in the visible with and without needle-to-shoot level clumping. In the near-infrared range with strong multiple scattering, mutual shadowing of needles within a shoots reduces the scattering coefficient of shoots and thus surface albedo, and increases total transmittance except for large solar zenith angles. Absorption does not change much due to needle-to-shoot level clumping except at large solar

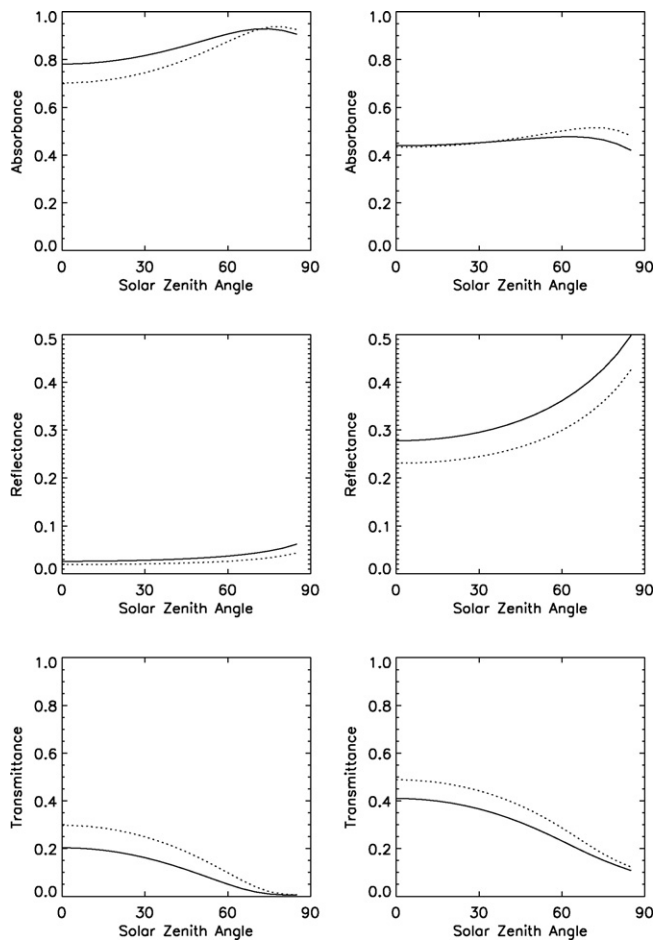


Fig. 12. Comparison of accumulated absorbance, reflectance and transmittance in the clear sky condition with (dashed line) and without (solid line) the needle-to-shoot level clumping in visible spectrum (left column) and near-infrared spectrum (right column).

zenith angles when multiple scattering is strong. Needle-to-shoot level clumping increases absorption at large solar zenith angles due to the reduced albedo. This result is consistent with what was shown using a ray-tracing model (Rochdi et al., 2006). Of course, the impact will vary according to how the needle-to-shoot area ratio varies by species.

4. Discussion and conclusions

This study presents a simple analytical geometric optical and radiative transfer (GORT) approach to model the light interaction with plant canopies. This model has advantages relative to current widely used two-stream schemes in providing better radiation estimation for photosynthesis by integrating a well-described statistical vertical foliage profile and the prognostic clumping factor, which account for the impact of both vertical and horizontal structure heterogeneity on radiative transfer in complex canopies.

This study provides an analytical GORT model, the ACTS, derived from the original version by Li et al. (1995) for the radiation over discontinuous plant canopies, with the following features. First, the analytical GORT has a slightly different assumption from the full GORT model. Tree crowns may overlap in the full GORT, but not in the analytical GORT. Non-overlapping of crowns is closer to the spatial distribution as observed in nature. The incorporation of the branch-scale clumping effect is included in the ACTS for needleleaf trees, which has a small effect but is theoretically sound and may prove important when coupled to a DGVM. The

application of a single canopy-scale clumping factor for all canopy layers was found sufficient to approximate vertical profiles of gap probability while preserving the total transmittance to the ground. Second, the ACTS model includes the effect of stem area (branches and trunk), which is critical for simulating radiative transfer during winter for deciduous trees. Third, ACTS also calculates sunlit and shaded leaf components. Fourth, an analytical approximation of the radiative transfer equation is used instead of the numerical method in the original full GORT model so that light transmittance, absorption and reflectance are calculated by a few simple formulae, which significantly reduces the computational cost compared to iterative multiple scattering schemes (a check of computational time for the full GORT versus the ACTS showed a reduction in time by more than 90%), such that this scheme is suitable for coupling with land surface models and GCMs. Using this approach the radiation interaction within and between discontinuous plant canopies is modeled as a function of the solar zenith angle, the tree geometry parameters, as well as the spectral properties of the canopy elements and the background.

Model simulations show that the model captures the main features of the PAR transmittance of discontinuous plant canopies, including the vertical sigmoid shape and hockey stick with the change of solar zenith angle, and the performance of the model with the predicted foliage clumping factor is much more reasonable than without the clumping factor.

This model has been shown to compare favorably to measurements of transmittance in a companion paper by Yang et al. (2010). Future work will involve the validation of the model for absorbance and reflectance. The impact of clumping on albedo, photosynthesis, competition and snowmelt will be evaluated in the Ent DGTEM. Also, with the advent of recent LIDAR satellite data that will provide global datasets of vegetation height structure (Lefsky et al., 2005), evaluation or parameterization of these height-structured DGVMs at the global scale is now becoming possible.

Acknowledgements

The work is supported by the NASA Modeling, Analysis, and Prediction (MAP) program under contract NNX06AD06G. We thank two reviewers for their valuable comments on this paper.

Appendix A.

Case 1: all trees have the same crown central height. In this case, identical trees of ellipsoid shape with horizontal and vertical crown radii r and b , respectively, are randomly distributed horizontally in space with crown count density λ , and the center of the crowns is at a single height, h . The statistical projected foliage area density profile is then,

$$\text{When } \frac{z-h}{b} \leq 1 : \frac{dL(z)}{dz} = \left\{ \lambda F_a \pi \cdot r^2 \left(1 - \left(1 - \left(\frac{z-h}{b} \right)^2 \right) \right) \right\}, \quad (\text{A1})$$

$$\text{Otherwise when } \frac{z-h}{b} > 1 : \frac{dL(z)}{dz} = 0. \quad (\text{A2})$$

Case 2: tree heights vary randomly. Identical trees with respect to crown dimension have an ellipsoid shape, with horizontal and vertical crown radii r and b , respectively; the trees are randomly distributed in space with crown count density λ ; the mean vertical center of the crowns is uniformly located between lower- and upper-bounds of crown center height h_1 and h_2 . The statistical projected foliage area density profile, $dL(z)/dz$, is then:

When $h_2 - b \leq h_1 + b$:

$$\begin{aligned} &\lambda F_a \pi \cdot r^2 \frac{(z+b-h_1)^2(h_1+2b-z)}{3b^2(h_2-h_1)}, \quad (h_1-b \leq z \leq h_2-b) \\ &\lambda F_a \pi \cdot r^2 \frac{3b^2-(h_2-h_1)^2-3(z-h_2)(z-h_1)}{3b^2}, \quad (h_1+b \leq z \leq h_2-b), \\ &\lambda F_a \pi \cdot r^2 \frac{(h_2-z+b)^2(2b+z-h_2)}{3b^2(h_2-h_1)}, \quad (h_1+b \leq z \leq h_2+b) \\ &0, \quad \text{otherwise} \end{aligned} \tag{A3}$$

Otherwise when $h_2 - b > h_1 + b$:

$$\begin{aligned} &\lambda F_a \pi \cdot r^2 \frac{(z+b-h_1)^2(h_1+2b-z)}{3b^2(h_2-h_1)}, \quad (h_1-b \leq z \leq h_2-b) \\ &\lambda F_a \pi \cdot r^2 \frac{4}{3} \frac{b}{h_2-h_1}, \quad (h_1+b \leq z \leq h_2-b) \\ &\lambda F_a \pi \cdot r^2 \frac{(h_2-z+b)^2(2b+z-h_2)}{3b^2(h_2-h_1)}, \quad (h_1+b \leq z \leq h_2+b) \\ &0, \quad \text{otherwise} \end{aligned} \tag{A4}$$

Note that DGVMs typically have cohorts of identical trees, and in the Ent DGTEM, such cohorts may be mixed together in a canopy. We describe the vertical layering scheme in a specific coupling with the Ent DGTEM in a later paper.

Appendix B.

We start from the work of Li and Strahler (1988), who derived expressions for the gap probability at the bottom of the canopy assuming that crowns do not intersect, $P_{\text{gap}}(0, \theta)$, for a given solar zenith angle θ :

$$P_{\text{gap}}(0, \theta) = \sum_{n=0}^{\infty} P_n(\theta) \int_0^{\infty} p(s|1) e^{-\tau_0 s} ds^n \tag{B1}$$

where $P_{\text{gap}}(0, \theta)$ is the gap probability for light passing through the whole canopy at the ground (0 height), given θ ; the attenuation parameter $\tau_0 = (G(\theta)L_t/\lambda V) = (3G(\theta)L_t/4\lambda\pi r^2 b)$; $P_n(\theta)$ is the gap probability of light rays passing through n crowns, given θ ; $p(s|1)$ is the distribution of the path length of rays passing through one crown; and $s|n$ is the distance of a photon traveling through n crowns.

Li and Strahler (1988) assume that the crowns are spheres and derived the formulae for $p(s|1) = (s/2r_2)$, giving,

$$q(\theta) = \int p(s|1) e^{-\tau_0 s} ds = \frac{1}{2\tau_0^2 r^2} [1 - (2\tau_0 r + 1)e^{-2\tau_0 r}] \tag{B2}$$

With the assumption of crowns randomly distributed in space, $P_n(\theta)$ follows the Poisson distribution (Li and Strahler, 1988 and Nilson, 1992):

$$P_n(\theta) = \frac{e^{-\lambda S(\theta)} (\lambda S(\theta))^n}{n!} \tag{B3}$$

where λ is the crown count density and $S(\theta)$ is the crown projected area on the ground along the ray direction with the incident zenith angle, θ (Li and Strahler, 1988), and $S(\theta) = \pi r^2 / \cos \theta$ for spherical crowns.

Then the gap probability at the bottom of the canopy for non-intersecting crowns is

$$P_{\text{gap}}(0, \theta) = \sum_{n=0}^{\infty} P_n(\theta) q^n = \sum_{n=0}^{\infty} \frac{e^{-\lambda S(\theta)} (\lambda S(\theta) q)^n}{n!} = e^{-\lambda S(\theta)(1-q(\theta))} \tag{B4}$$

With leaf area index $L_t = (4/3)\lambda\pi r^3 F_a$ for spherical crowns, Eq. (10) becomes,

$$P_{\text{gap}}(0, \theta) = \exp\left(-\frac{3GL_t(1-q(\theta))}{4\tau r \cdot \cos \theta}\right) = \exp\left(-\frac{\gamma GL_t}{\cos \theta}\right) \tag{B5}$$

Thus the clumping factor is:

$$\gamma = \frac{3}{4\tau_0 r} \left(1 - \frac{1 - (2\tau_0 r + 1)e^{-2\tau_0 r}}{2\tau_0^2 r^2}\right) \tag{B6}$$

where $\tau_0 r = (3GL_t/4\lambda\pi r^2)$ for spherical crowns.

References

Albani, M., Medvigy, D., Hurtt, G.C., Moorcroft, P.R., 2006. The contributions of land-use change, CO₂ fertilization, and climate variability to the Eastern US carbon sink. *Glob. Change Biol.* 12 (12), 2370–2390.

Anderson, M.C., Norman, J.P., Kustas, W.P., Li, F.Q., Prueger, J.H., Mecikalski, J.R., 2005. Effects of vegetation clumping on two-source model estimates of surface energy fluxes from an agricultural landscape during SMACEX. *J. Hydrometeorol.* 6 (6), 892–909.

Asrar, G., Myneni, R.B., Choudhury, B.J., 1992. Spatial heterogeneity in vegetation canopies and remote sensing of absorbed photosynthetically active radiation: a modeling study. *Remote Sens. Environ.* 41, 85–103.

Barford, C.C., Wofsy, S.C., Goulden, M.L., Munger, J.W., Pyle, E.H., Shawn, P., Urbanski, S.P., Hutyrka, L., Saleska, S.R., Fitzjarrald, D., Moore, K., 2001. Factors controlling long- and short-term sequestration of atmospheric CO₂ in a mid-latitude forest. *Science* 294 (5547), 1688–1691, doi:10.1126/science.1062962.

Baldocchi, D.B., Collineau, S., 1994. The physical nature of solar radiation in heterogeneous canopies: spatial and temporal attributes. In: Caldwell, M.M., Pearcy, R.W., San Diego (Eds.), *Exploitation of Environmental Heterogeneity by Plants*. Academic Press, pp. 21–71.

Bonan, G.B., 1996. A land surface model (LSM Version 1.0) for ecological, hydrological, and atmospheric studies: technical description and user's guide. National Center of Atmospheric Research, Boulder, Colorado, p. 122.

Bonan, G.B., Levis, S., Kergoat, L., Oleson, K.W., 2002. Landscapes as patches of plant functional types: an integrating concept for climate and ecosystem models. *Glob. Biogeochem. Cycles* 16, 1021, doi:10.1029/2000GB001360.

Cescatti, A., 1997a. Modelling the radiative transfer in discontinuous canopies of asymmetric crowns. I. Model structure and algorithms. *Ecol. Model.* 101, 263–274.

Cescatti, A., 1997b. Modelling the radiative transfer in discontinuous canopies of asymmetric crowns. II. Model testing and application in a Norway spruce stand. *Ecol. Model.* 101, 275–284.

Chen, J.M., Black, T.A., 1991. Measuring leaf area index of plant canopies with branch architecture. *Agric. Forest Meteorol.* 57, 1–12.

Chen, J.M., Cihlar, J., 1995. Quantifying the effect of canopy architecture on optical measurements of leaf area index using two gap size analysis methods. *IEEE Trans. Geosci. Remote Sens.* 33, 777–787.

Chen, J.M., 1996. Optically-based methods for measuring seasonal variation in leaf area index of boreal conifer forests. *Agric. Forest Meteorol.* 80, 135–163.

Chen, Q., Baldocchi, D., Gong, P., Dawson, T., 2008. Modeling radiation and photosynthesis of a heterogeneous savanna woodland landscape with a hierarchy of model complexities. *Agric. Forest Meteorol.* 148 (6–7), 1005–1020.

Cox, P.M., 2001. Description of the “TRIFFID” Dynamic Global Vegetation Model. Hadley Centre, London, 16.

Dai, Y., Dickinson, R.E., Wang, Y.P., 2004. A two-big-leaf model for canopy temperature, photosynthesis, and stomatal conductance. *J. Climate* 17 (6), 2281–2299.

Davi, H., Bouriaud, O., Dufrene, E., Soudani, K., Pontailier, J.Y., Le Maire, G., Francois, C., Breda, N., Granier, A., Le Dantec, V., 2006. Effect of aggregating spatial parameters on modelling forest carbon and water fluxes. *Agric. Forest Meteorol.* 139 (3–4), 269–287.

Dickinson, R.E., 1983. Land surface processes and climate—surface albedos and energy balance. *Adv. Geophys.* 25, 305–353.

Dickinson, R., Henderson-Sellers, A., Kennedy, P., Wilson, M., 1986. Biosphere-Atmosphere Transfer Scheme (BATS) for the NCAR community climate model. Technical note, NCAR/TN-275+STR.

Enquist, B.J., Niklas, K.J., 2001. Invariant scaling relations across tree-dominated communities. *Nature* 410 (6829), 655–660.

Hardy, J.P., Davis, R., Jordan, R., Li, X., Woodcock, C.E., Ni, W., McKenzie, J., 1997. Snow Ablation modeling at the stand scale in a boreal jack pine forest. *J. Geophys. Res.* 102 (D24), 29397–29406.

Jonckheere, I., Fleck, S., Nackaerts, K., Muys, B., Coppin, P., Weiss, M., Baret, F., 2004. Review of methods for in situ leaf area index determination. Part I. Theories, sensors and hemispherical photography. *Agr. Forest Meteorol.* 121, 19–35.

Jupp, D.L.B., 2004. Imaging, scene and image models and geostatistics. In: *EOC Annual Science Meeting*, 25pp.

Kenkel, N.C., 1988. Pattern of self-thinning in jack pine: testing the random mortality hypothesis. *Ecology* 69 (4), 1017–1024.

Kiang, N.Y., 2002. Savannas and seasonal drought: The landscape-leaf connection through optimal stomatal control. Environmental Science, Policy and Management. Berkeley, University of California at Berkeley, Dissertation, 303 pp.

- Kiang, N.Y., Koster, R.D., Moorcroft, P.R., Ni-Meister, W., Rind, D., 2006. Ent: A Dynamic Global Terrestrial Ecosystem Model for Coupling with GCMs, EOS Transactions, American Geophysical Union, 87(52), Fall Meeting Supplement, Abstract B51A-0301.
- Knyazikhin, Y., Martonchik, J.V., Myneni, R.B., Diner, D., Running, S.W., 1998. Synergistic algorithm for estimating vegetation canopy leaf area index and fraction of absorbed photosynthetically active radiation from MODIS and MISR data. *J. Geophys. Res.* 103, 32257–32276.
- Krinner, G., Viovy, N., de Noblet-Ducoudré, N., Ogée, J., Polcher, J., Friedlingstein, P., Ciais, P., Sitch, S., Prentice, I.C., 2005. A dynamic global vegetation model for studies of the coupled atmosphere-biosphere system. *Global Biogeochem. Cycles* 19, GB1015, doi:10.1029/2003GB002199.
- Kucharik, C.J., Norman, J.M., Gower, S.T., 1999. Characterization of radiation regimes in nonrandom forest canopies: theory, measurements, and a simplified modeling approach. *Tree Physiol.* 19, 695–706.
- Lang, A.R.G., 1991. Application of some of Cauchy's theorems to estimation of surface areas of leaves, needles and branches of plants, and light transmittance. *Agric. Forest Meteorol.* 55, 191–212.
- Law, B.E., Cescatti, A., Baldocchi, D.D., 2001. Leaf Area Distribution and Radiative Transfer in Open-canopy Forests: Implications for Mass and Energy Exchange. Heron Publishing.
- Leblanc, S.G., Chen, J.M., White, H.P., Latifovic, R., Lacaze, R., Roujean, J.L.R., 2005. Canada-wide foliage clumping index mapping from multiangular POLDER measurements. *Can. Aeronaut. Space Inst.*
- Lefsky, M.A., Harding, D.J., Keller, M., Cohen, W.B., Carabajal, C.C., Espirito-Santo, F.D.B., Hunter, M.O., de Oliveria Jr., R., 2005. Estimates of forest canopy height and aboveground biomass using ICESat. *Geophys. Res. Lett.* 32, L22S02.
- Leuning, R., Dunin, F.X., Wang, Y.-P., 1998. A two-leaf model for canopy conductance, photosynthesis and partitioning of available energy. II. Comparison with measurements. *Agric. Forest Meteorol.* 91, 113–125.
- Levis, S., Bonan, G.B., Versteinstein, M., Oleson, K.W., 2004. The Community Land Model's Dynamic Global Vegetation Model (CLM-DGVM): Technical Description and User's Guide. Boulder, Colorado, Terrestrial Sciences Section Climate and Global Dynamics Division. National Center for Atmospheric Research.
- Li, X., Strahler, A.H., 1988. Modeling the gap probability of a discontinuous vegetation canopy. *IEEE Trans. Geosci. Remote Sens.* 26 (2), 161–170.
- Li, X., Strahler, A.H., Woodcock, C.E., 1995. A hybrid geometric optical-radiative transfer approach for modeling albedo and directional reflectance of discontinuous canopies. *IEEE Trans. Geosci. Remote Sens.* 33 (2), 466–480.
- Matthews, E., 1983. Global vegetation and land use: new high-resolution data bases for climate studies. *J. Appl. Meteorol.* 22, 474–487.
- Mo, X.G., Chen, J.M., Ju, W.M., Black, T.A., 2008. Optimization of ecosystem model parameters through assimilating eddy covariance flux data with an ensemble Kalman filter. *Ecol. Model.* 217 (1–2), 157–173.
- Moeur, M., 1997. Spatial models of competition and gap dynamics in old-growth Tsuga heterophylla/Thuja plicata forests. *Forest Ecol. Manage.* 94, 175–186.
- Moorcroft, P., Hurtt, G.C., Pacala, S.W., 2001. A method for scaling vegetation dynamics: The ecosystem demography model (ED). *Ecol. Monogr.* 71 (4), 557–586.
- Ni, W.G., Li, X.W., Woodcock, C.E., Roujean, J.L., Davis, R.E., 1997. Transmission of solar radiation in boreal conifer forests: measurements and models. *J. Geophys. Res.* 102 (D24), 29555–29566.
- Ni, W.G., Li, X.W., Woodcock, C.E., Caetano, M.R., Strahler, A.H., 1999a. An analytical hybrid GORT model for bidirectional reflectance over discontinuous plant canopies. *IEEE Trans. Geosci. Remote Sens.* 37 (2), 987–999.
- Ni, W., Woodcock, C.E., Jupp, D.L.B., 1999b. Variance in bidirectional reflectance over discontinuous plant canopies. *Remote Sens. Environ.* 69 (1), 1–15.
- Ni, W., Woodcock, C.E., 2000. Effect of canopy structure and the presence of snow on the albedo of boreal conifer forest. *J. Geophys. Res.* 105 (D9), 11879–11888.
- Ni, W., Jupp, D.L.B., 2000. Spatial Variance in directional remote sensing imagery—recent developments and future perspectives. *Remote Sens. Rev.* 18 (2–4), 441–479.
- Ni, W., Li, X., 2000. A coupled vegetation – soil bidirectional reflectance model for a semi-arid landscape. *Remote Sens. Environ.* 74, 113–124.
- Ni-Meister, W., Jupp, D.L.B., Dubayah, R., 2001. Modeling lidar waveforms in heterogeneous and discrete canopies. *IEEE Trans. Geosci. Remote Sens.* 39 (9), 1943–1958.
- Ni-Meister, W., Strahler, A.H., Woodcock, C.E., Schaaf, C., Jupp, D.L.B., Yao, T., Zhao, F., Yang, X., 2008. Modeling the hemispherical scanning, below-canopy lidar and vegetation structure characteristics with a geometric-optical and radiative transfer model. *Can. J. Remote Sens.* 34 (S2), S385–S397.
- Nilson, T., 1971. A theoretical analysis of the frequency of gaps in plant stands. *Agric. Forest Meteorol.* 8, 25–38.
- Nilson, T., 1992. Radiative transfer in nonhomogeneous plant canopies. *Adv. Bioclimatol.* 1, 59–88.
- Nilson, T., Kuusk, A., 2004. Improved algorithm for estimating canopy indices from gap fraction data in forest canopies. *Agric. Forest Meteorol.* 124, 157–169.
- Oker-Blom, P., Smolander, H., 1988. The ratio of shoot silhouette area to total needle area in Scots pine. *For. Sci.* 34, 894–906.
- Oker-Blom, P., Kellomaki, S., Smolander, H., 1983. Photosynthesis of a Scots pine shoot: the effect of shoot inclination on the photosynthetic response subjected to direct radiation. *Agric. Forest Meteorol.* 29, 191–206.
- Oker-Blom, P., Lappi, J., Smolander, H., 1991. Radiation regime and photosynthesis of coniferous stands. In: Myneni, R.B., Ross, J. (Eds.), *Photon-Vegetation Interactions—Application in Optical Remote Sensing and Plant Ecology*. Springer-Verlag, New York.
- Pacala, S.W., Hurtt, G.C., Baker, D., Peylin, P., Houghton, R.A., Birdsey, R.A., Heath, L., Sundquist, E.T., Stallard, R.F., Ciais, P., Moorcroft, P., Caspersen, J.P., Shevliakova, E., Moore, B., Kohlmaier, G., Holland, E., Gloor, M., Harmon, M.E., Fan, S.-M., Sarmiento, J.L., Goodale, C.L., Schimel, D., Field, C.B., 2001. Consistent land-and atmosphere-based US carbon sink estimates. *Science* 292, 2316–2320, doi:10.1126/science.1057320.
- Rochdi, N., Fernandes, R., Chelle, M., 2006. An assessment of needles clumping within shoots when modeling radiative transfer within homogeneous canopies. *Remote Sens. Environ.* 102, 116–134.
- Ross, J.K., 1975. Radiative transfer in plant communities. In: Monteith, J.L. (Ed.), *Vegetation and the Atmosphere*, volume 1: Principles. Academic Press, London, p. 278.
- Ross, J.K., 1981. The Radiative Regime and Architecture of Plant Stands, 391 pp., Dr. W. Junk, Kluwer Academic Publishers, Norwell, MA.
- Sellers, P.J., 1985. Canopy reflectance, photosynthesis and transpiration. *Int. J. Remote Sens.* 74, 125–144.
- Sellers, P.J., Randall, D.A., Gollatz, G.J., Berry, J.A., Field, C.B., Dazlich, D.A., Zhang, C., Collole, G.D., Bounoua, L., 1996. A revised land surface parameterization (SiB₂) for atmospheric GCMs. Part I: Model formulation. *J. Climate* 9, 676–705.
- Sitch, S., Smith, B., Prentice, I.C., Arneth, A., Bondeau, A., Cramer, W., Kaplan, J.O., Levis, S., Lucht, W., Sykes, M.T., Thonicke, K., Venevsky, S., 2003. Evaluation of ecosystem dynamics, plant geography and terrestrial carbon cycling in the LPJ dynamic global vegetation model. *Glob. Change Biol.* 9, 161–185.
- Smolander, S., Stenberg, P., 2003. A method to account for shoot scale clumping in coniferous canopy reflectance models. *Remote Sens. Environ.* 88, 363–373.
- Song, C., Woodcock, C.E., 2002. The spatial manifestation of forest succession in optical imagery—the potential of multiresolution imagery. *Remote Sens. Environ.* 82 (2–3), 271–284.
- Song, C., Woodcock, C.E., 2003. Monitoring forest succession with multitemporal Landsat images: factors of uncertainty. *IEEE Trans. Geosci. Remote Sens.* 41 (11), 2557–2567.
- Song, C., Woodcock, C.E., Li, X., 2002. The spectral/temporal manifestation of forest succession in optical imagery—the potential of multitemporal imagery. *Remote Sens. Environ.* 82 (2/3), 285–302.
- Spitters, C.J.T., 1986. Separating the diffuse and direct components of global radiation and its implications for modeling canopy photosynthesis. Part II: Calculation of canopy photosynthesis. *Agric. Forest Meteorol.* 38, 231–242.
- Valladares, F., Guzman, B., 2006. Canopy structure and spatial heterogeneity of understory light in an abandoned Holm oak woodland. *Ann. Forest Sci.* 63, 749–761.
- Walcroft, A.S., Brown, K.J., Schuster, W.S.F., Tissue, D.T., Turnbull, M.H., Griffin, K.L., Whitehead, D., 2005. Radiative transfer and carbon assimilation in relation to canopy architecture, foliage area distribution and clumping in a mature temperate rainforest canopy in New Zealand. *Agric. Forest Meteorol.* 135 (1–4), 326–339.
- Wang, Y.P., 2003. A comparison of three different canopy radiation models commonly used in plant modeling. *Funct. Plant Biol.* 30, 143–152.
- Wang, Y.P., Jarvis, P.G., 1990a. Description and validation of an array model—MAESTRO. *Agric. Forest Meteorol.* 51, 257–280.
- Wang, Y.P., Jarvis, P.G., 1990b. Influence of crown structural properties on PAR absorption, photosynthesis and transpiration in sitka spruce: application of a model (MAESTRO). *Tree Physiol.* 7, 297–316.
- Wang, Y.P., Jarvis, P.G., Benson, M.L., 1990. Two-dimensional needle-area density distribution within the crowns of Pinus radiata. *Forest Ecol. Manage.* 32, 217–237.
- Wang, Y.P., Jarvis, P.G., 1993. Influence of shoot structure on the photosynthesis of sitka spruce (Picea sitchensis (Bong.) Carr.). *Funct. Ecol.* 7, 433–451.
- Wang, Y.-P., Leuning, R., 1998. A two-leaf model for canopy conductance, photosynthesis and partitioning of available energy. I: Model description and comparison with a multi-layer model. *Agric. Forest Meteorol.* 91, 89–111.
- West, G.B., Brown, J.H., Enquist, B.J., 1999. A general model for the structure and allometry of plant vascular systems. *Nature* 400, 664–667.
- Yang, R., Friedl, M.A., Ni, W., 2001. Parameterization of shortwave radiation fluxes for nonuniform vegetation canopies in land surface models. *J. Geophys. Res.* 106 (D13), 14275–14286.
- Yang, W., Ni-Meister, W., Kiang, N.Y., Moorcroft, P., Strahler, A.H., Oliphant, A., 2010. A clumped-foliage canopy radiative transfer model for a global dynamic terrestrial ecosystem model. II: Comparison to measurements. *Agric. Forest Meteorol.*, doi:10.1016/j.agrformet.2010.02.008, this issue.